

## A diabatic and isothermal sound waves: the case of supercritical nitrogen

F. Bencivenga<sup>1</sup>, A. Cunsolo<sup>2</sup>, M. Kirsch<sup>1</sup>, G. Monaco<sup>1</sup>, G. Ruocco<sup>3</sup> and F. Sette<sup>1</sup><sup>1</sup> European Synchrotron Radiation Facility, B.P. 220 F-38043 Grenoble, Cedex France.<sup>2</sup> CRS SOFT-INFM-CNR -Operative Group in Grenoble c/o ILL, B.P. 220 F-38043 Grenoble, Cedex France.<sup>3</sup> Dipartimento di Fisica and CRS SOFT-INFM-CNR, Università di Roma "La Sapienza", Roma, Italy.

(Dated: March 23, 2024)

The acoustic sound dispersion of nitrogen in its liquid and supercritical phases has been studied by Inelastic X-Ray Scattering. Approaching supercritical conditions, the gradual disappearance of the positive sound dispersion, characteristic of the low temperature liquid, is observed. In the supercritical state, evidence for a crossover between adiabatic and isothermal sound propagation regimes is inferred by an analysis of the dynamic structure factor based on generalized hydrodynamics.

PACS numbers:

The development of Inelastic X-ray Scattering (IXS) [1, 2, 3, 4, 5] has opened up new opportunities in the study of the high-frequency dynamics of liquids at nanometer distances and picosecond timescales. Various IXS investigations unveiled that, in the proper thermodynamic conditions, structural relaxation processes occur in the THz frequency range. These processes manifest themselves by an upward bending of the sound dispersion relation, which deviate from the low-frequency linear behavior dictated by the adiabatic sound velocity. Accordingly, the sound velocity increases from the adiabatic value,  $c_s$ , to the "infinite" frequency value,  $c_\infty$  [2, 3, 4, 5, 6, 7, 8, 9, 10, 11, 12, 13, 14, 15, 16, 17, 18]. If  $\omega_L(Q)$  is the frequency of the probed acoustic excitation with wave vector  $Q$ , and  $\tau_L$  is the characteristic relaxation time of the structural relaxation process, the system exhibits a liquid-like (viscous) behavior if the condition  $\omega_L(Q) \ll 1/\tau_L$  is fulfilled: in this limit the dispersion relation is  $\omega_L(Q) = c_s Q$ . In the opposite limit, the elastic one, where  $\omega_L(Q) \gg 1/\tau_L$ , structural rearrangements are too slow to efficiently dissipate the energy of the acoustic waves: in this limit  $\omega_L(Q) = c_\infty Q$ . A schematic picture of this visco-elastic variation of the sound velocity from  $c_s$  to  $c_\infty$  is shown in Fig. 1a (full thick line), where the cross-over condition  $\omega_L(Q) = 1/\tau_L$  is indicated by the vertical arrow, and the adiabatic and infinite linear dispersion relations are indicated by the full and dashed lines respectively. Here the dash-dot line represents the value of  $\omega_L(Q) = 1/\tau_L$ , which is here assumed to be  $Q$ -independent.

The structural relaxation process, in principle, is not the only relaxation process that could affect the high frequency dynamics of a liquid. On general grounds, also other physical processes, as for example thermal diffusion, can modify the behavior of sound waves. In this case, given a thermal diffusion coefficient  $D_T$  and a thermal relaxation time  $\tau_T = 1/D_T Q^2$ , a modification of the sound velocity takes place around a crossover frequency given by  $\omega_L(Q) = D_T Q^2$ . In this case, for  $D_T Q^2 \ll \omega_L(Q)$  the thermal diffusion is much slower than the period of acoustic waves, which therefore propagate adiabatically, i.e. without any thermal exchange with the local environment. In the opposite

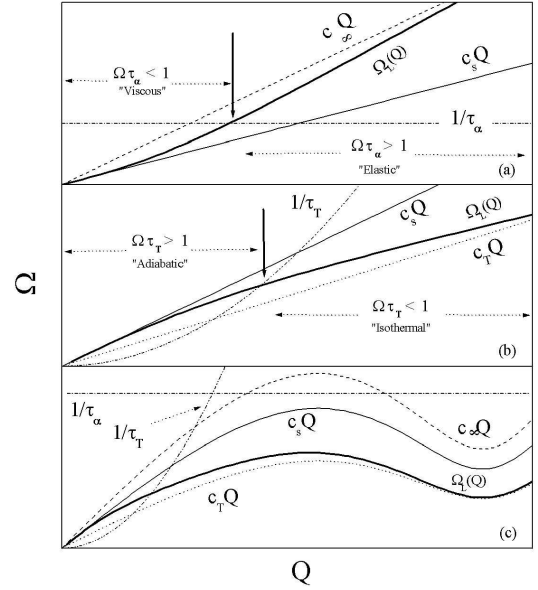


FIG. 1: Schematic representation of the various sound regimes highlighting the two cross-over conditions. Upper panel: viscoelastic transition taking place at  $\omega_L = 1/\tau_L$ ; middle panel: isothermal transition taking place at  $\omega_L = D_T Q^2$ ; bottom panel: realistic non linear dispersions under favorable experimental conditions for  $\omega_L = 1/\tau_L$  and  $\omega_L = D_T Q^2$ . Vertical arrows indicate the crossover regions as discussed in the text. The isothermal (dotted line), adiabatic (solid line), infinite frequency (dashed line) and apparent (thick solid line) sound dispersions are reported together with the relaxation frequency  $1/\tau_L$  (dash-dot line) and thermal frequency  $D_T Q^2$  (dashed-double dotted line).

limit,  $D_T Q^2 \gg \omega_L(Q)$ , the thermalization of the acoustic wave is instantaneous, and the effective propagation mechanism becomes isothermal with sound velocity  $c_T = c_s / \gamma$  ( $\gamma$  is the specific heat ratio). One therefore expects to observe a transition between the adiabatic and the isothermal regimes when  $\omega_L(Q) = D_T Q^2$ . This case is schematically presented in Figure 1b, where linear lines represent the adiabatic (full line) and isothermal

(dotted line) sound dispersion, and the dash-dot-dot line indicates the  $Q$  dependence of  $l = \tau(Q)$ .

Contrary to the visco-elastic transition, which has been experimentally documented in many liquids [4, 5, 6, 7, 8, 9, 10, 11, 12, 13, 14, 15, 16, 17, 18], no firm evidence of the adiabatic to isothermal transition is available. This is mainly due to the following reasons: i) The amplitude of the dispersive effect between  $c_s$  and  $c_T$  is proportional to

$1$  which, in most liquids, is close to zero. ii) The effect is often completely masked by the competing visco-elastic transition. iii) The crossover occurs typically at large  $Q$ , often above the position of the first sharp diffraction peak (FSDP) of the static structure factor,  $S(Q)$ . Here, however, the finite- $Q$  generalization of the isothermal sound speed  $c_T(Q)$  - which is proportional to  $1/S(Q)^{1/2}$  - [19], becomes too small to be reliably extracted from the measured  $S(Q; \omega)$  spectra.

These obstacles to the observation of the adiabatic to isothermal sound propagation transition can be reduced close to supercritical conditions for the following reasons: i) the competing positive dispersion induced by the viscoelastic transition is expected to be much weaker. ii) The crossover condition for the viscoelastic transition is expected to move at higher  $Q$ , i.e. higher frequency, since the structural rearrangements occur on shorter time scales. iii) Moreover, the intensity of the FSDP is much weaker, and consequently  $c_T(Q)$  does not display any longer a pronounced minimum in the vicinity of the FSDP. iv) Finally, the sound speed decreases on approaching the critical point, and therefore the transition will move towards smaller  $Q$  values. This scenario is schematically pictured in Figure 1c, where the combined effects of the structural and thermal relaxation processes are modelled within the framework of the molecular hydrodynamics [19]. The values of  $\omega$  and  $\tau(Q)$  are chosen such that the transition is actually determined by the thermal relaxation process, as indicated by the arrow.

This letter, guided by the above considerations, reports an IXS study of liquid and supercritical nitrogen. Nitrogen has been chosen because the two thermodynamic regimes (liquid and supercritical) can be easily obtained within an experimentally accessible pressure and temperature range, and because of its favorable inelastic scattering cross section. Figure 2 shows the portion of the explored thermodynamic plane. The inset reports the expected  $Q$ -values,  $Q(T)$ , for which the crossover from the adiabatic to the isothermal regime should occur:  $Q(T) = c_s = D_T$ . The values of  $c_s$  and  $D_T$  were obtained from the nitrogen Equation-of-State (EoS) [20].

The experiment was performed on ID 28 at the European Synchrotron Radiation Facility (ESRF). The beam-line was set up with an instrumental resolution function of 1.5 meV full-width-half-maximum (FWHM). The sample was embedded in a large volume, high pressure cell kept in thermal contact with the cold finger of a cryostat. The optical windows were two 1 mm thick diamond disks, and the sample length amounted to 10 mm. The pressure stability was better than 5 bar over the ac-

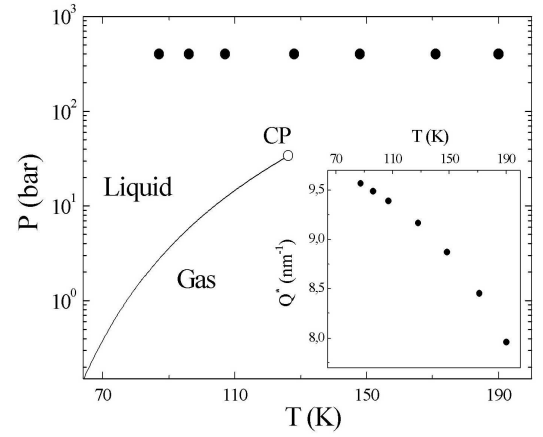


FIG. 2: Phase diagram of nitrogen. The investigated thermodynamic points are reported as full circles. The solid line represents the coexistence curve, ending at the critical point CP ( $T_c = 126.2$  K,  $P_c = 34$  bar,  $\rho_c = 0.313$  g/cm<sup>3</sup>). In the inset we report the expected  $Q$ -values for the isothermal transition for the sound propagation, as estimated from the nitrogen equation-of-state using  $Q = c_s = D_T$ .

quisition time of a typical spectrum. IXS spectra were recorded following an isobaric path at 400 bar from sub-critical to supercritical conditions (full dots in figure 2). Cell contribution as determined by empty cell measurement yielded a negligible contribution to the signal for all exploited scattering geometries. Multiple scattering has been estimated to be negligible. The recorded signal is therefore proportional to the dynamic structure factor,  $S(Q; \omega)$ , convoluted with the instrumental resolution function.

The data analysis has been performed using a line-shape model derived within the framework of the memory function formalism [19]. In this model the dynamic structure factor is written as:

$$S(Q; \omega) = \frac{\hbar}{K_B T} [\ln(\omega) + 1] \text{Im} [L^2 - Q^2 c_T^2 - i l m_Q(\omega)]^{-1} \quad (1)$$

where  $n(\omega)$  is the Bose factor and  $m_Q(\omega)$  is the Fourier transform of the time dependent memory function [7, 8, 19], which has been approximated by:

$$m_Q(t) = c_T^2(Q) [c_T^2(Q) - 1] Q^2 e^{D_T(Q) Q^2 t} + [c_1^2(Q) - c_s^2(Q)] Q^2 e^{-\Gamma(Q)t} + \gamma^2(Q) t \quad (2)$$

Following the prescriptions of molecular hydrodynamics, all the thermodynamic quantities entering Eq. 2 are assumed as  $Q$  dependent extensions of their respective macroscopic counterparts.

The function in Eq. 2 accounts for the fast dynamics which induces an instantaneous time decay of  $m_Q(t)$

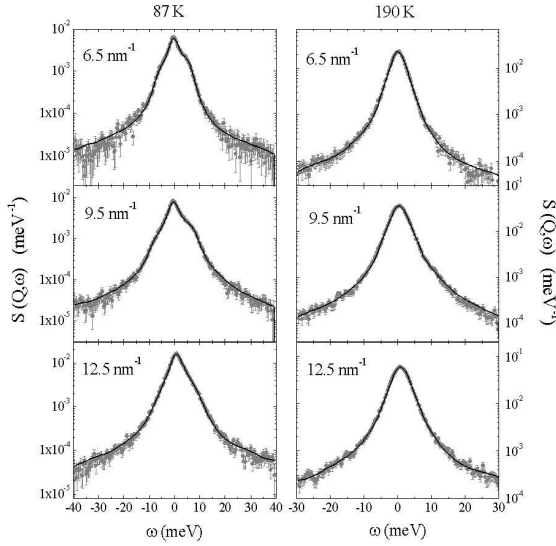


FIG. 3: Selection of IXS spectra of liquid nitrogen at  $P = 400$  bar and two temperatures (87 K and 190 K) at momentum transfers as indicated in the individual panels. The experimental data (full circles) are reported together with their best lineshapes (solid lines).

[7, 8]. The second exponential term of Eq. 2 accounts for the viscoelastic transition that disperses the sound velocity, with increasing  $Q$ , from its low to its high frequency limiting value,  $c_s(Q)$  and  $c_l(Q)$  respectively. Finally, the first term in Eq. 2 accounts for the thermal diffusion process. In the low- $Q$  limit the thermal part of the memory function yields a central peak in the spectral density, whose integrated intensity is proportional to  $(Q)^{-1}$ , and its halfwidth is given by  $D_T(Q)Q^2$ . Consequently the proposed model predicts the "classical" hydrodynamics description at low  $Q$ .

The experimental data are described by the convolution of the model reported in Eqs 1 and 2 with the experimentally determined instrument resolution function. In the fitting procedure, the parameters  $(Q)$ ,  $c_l(Q)$ ,  $c_s(Q)$  and an overall intensity factor  $A$  are left as free parameters. Owing to the lack of experimental or computational results on the  $Q$ -dependence of  $\Gamma$  and  $D_T$ , these variables have been fixed to their thermodynamic  $(Q \rightarrow 0)$  values, as derived from the EoS of nitrogen [20]. The parameters  $c_l(Q)$  and  $c_s(Q)$  have been fixed to the values calculated through [19]:

$$c_l(Q) = \Gamma^{-1/2} c_s(Q) = \left[ \frac{K_B T}{M S(Q)} \right]^{1/2} \quad (3)$$

where  $K_B$  and  $M$  are the Boltzmann constant and the molecular mass of nitrogen, respectively. The static structure factor  $S(Q)$  was determined experimentally by recording the energy-integrated scattering, corrected for the known nitrogen form factor,  $f(Q)$  [21], as well as for all geometrical artifacts. In order to put  $S(Q)$  on an

absolute scale, we have normalized the measured intensity to fulfill the compressibility constraint in the  $Q = 0$  limit. Finally, the apparent sound velocity of acoustic excitations,  $c_l(Q)$ , has been determined using the relation  $c_l(Q) = \Gamma^{-1/2}(Q)Q$ , where  $\Gamma^{-1/2}(Q)$  is the frequency value of the maximum of the longitudinal current spectra,  $\Gamma^{-1/2}(Q) = Q^2$ .

Selected IXS spectra and their best fits are shown in Fig. 3. Each spectrum typically covers an energy transfer range of  $\sim 40$  meV and was collected in the  $2$  to  $14$  nm $^{-1}$   $Q$  range. The logarithmic plot emphasizes the overall good agreement between experimental and model line shapes, even in the tails of the spectra.

The comparisons between the apparent dispersion relation,  $\Gamma^{-1/2}(Q)$  vs:  $Q$  (open circles), and both isothermal (dotted line) and adiabatic (full line) ones, are shown in Fig. 4 at the four different temperatures 87, 128, 171, and 191 K. In the same figure we also report the infinite frequency dispersion relation (fulldots) and the inverse of the structural relaxation time  $\Gamma^{-1}(Q)$  (dashed-dot line) as derived from the best fit result. The inverse of the thermal relaxation time,  $D_T Q^2$ , is also reported as derived from the nitrogen EoS (dash-dot-dot line). The results of Fig. 4a, corresponding to the lowest investigated temperature (87 K), show that the apparent dispersion is systematically higher than the adiabatic one. Although the  $c_l$  limit is not completely reached, in this thermodynamic point the high frequency dynamics of the liquid is mostly influenced by the structural relaxation process. This influence is considerably weaker at  $T = 128$  K (Panel b) due to the higher value of  $\Gamma^{-1}(Q)$  which prevents even more to reach the viscoelastic crossover conditions. On further increase of the temperature (Panel c and d),  $\Gamma^{-1}(Q)$  moves definitively out of the probed frequency range and any hint of positive dispersion on the sound velocity disappears. In fact, with increasing temperature the apparent dispersion relation initially approaches the adiabatic sound dispersion, but at the highest temperature is observed to go below the adiabatic dispersion and to approach the isothermal one: this is the onset of the expected transition between adiabatic and isothermal regimes. This effect is most clearly seen for the three highest  $Q$  points between  $9.5$  and  $14$  nm $^{-1}$ .

The arrows in Figure 4 (panels c and d) indicate the  $Q$  points where one would expect the adiabatic-isothermal transition ( $\Gamma^{-1/2}(Q) = D_T Q^2$ , left arrows) and where the transition actually occurs (right arrows): a  $Q$  value definitively higher than the one estimated by the left arrow. This difference between expected and observed transition  $Q$  points is an indication of the  $Q$ -dependence of the parameter  $D_T$ , which we neglected so far. This behavior is in agreement with the expectations suggested by numerical simulations of various molecular liquids [22, 23] pointing to a monotonic decrease of  $D_T(Q)$  with increasing  $Q$ . As a consequence, the position of the crossover is shifted towards higher momentum transfers. Even though the transition to the isothermal regime is not fully completed, its occurrence is inferred from this system-

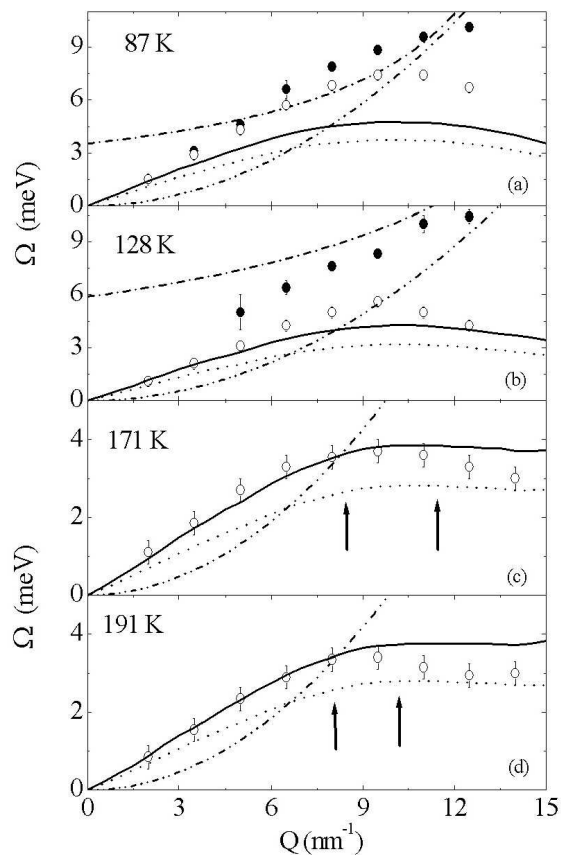


FIG. 4: Dispersion curves of the longitudinal acoustic mode of nitrogen at 87, 128, 171 and 190 K. The full and dotted lines represent the adiabatic and isothermal dispersions, derived from  $S(Q)$  measurements, as discussed in the text; the open circles indicate the maxima of longitudinal current spectra. The dash-dotted and dash-double dotted lines represent  $1 = c(Q)$  and  $D_T Q^2$ , respectively; the former has been evaluated interpolating the results of the performed lineshape analysis, which allowed also to extract the values of in finite-frequency sound dispersion, reported as full circles.

atic trend. Furthermore, it is worthwhile recalling that the present results have been obtained without imposing any constraint on the lineshaping parameters. Moreover, the values of the isothermal sound dispersions have been determined independently through the measured  $S(Q)$ .

In conclusion our observations can be summarized as follows: i) the apparent sound branch of nitrogen shows clear signatures of a positive sound dispersion in the liquid phase, thus witnessing the presence of a structural relaxation process. ii) The positive sound dispersion gradually disappears while reaching supercritical conditions, most likely due to the shift of  $1 = c(Q)$  above the  $1 = c_L(Q)$  values. iii) At the highest investigated temperatures, the transition from the adiabatic to the isothermal sound propagation is observed.

These findings indicate that, in the liquid phase, the high frequency dynamics of a simple, non-associated fluid, such as nitrogen, is mainly ruled by the structural relaxation, as manifested by the positive sound dispersion. In contrast, in the supercritical phase, the role of the structural relaxation becomes negligible and the most evident dispersive effect is the bending down of the apparent dispersion, from its adiabatic value to the isothermal one. In this regime, the thermal relaxation process rules the high frequency dynamics.

#### I. ACKNOWLEDGMENTS

We are grateful to Dr. T. Scopigno for critical reading of the manuscript. We are also grateful to D. Gambetti and R. Verbeni for help in the preparation of the experiment.

- 
- [1] E. Burkel, *Inelastic Scattering of X-Rays with Very High Energy Resolution* (Springer-Verlag, Berlin, 1991)
  - [2] F. Sette et al., *Phys. scr. T* 66, 48-56 (1996)
  - [3] E. Burkel, *Rep. Prog. Phys.* 63, 171 (2000)
  - [4] G. Ruocco and F. Sette, *J. Phys.: Condens. Matter* 11, R259 (1999)
  - [5] T. Scopigno et al., *Rev. Mod. Phys.* 77, 881 (2005)
  - [6] A. Cunsolo et al., *J. Chem. Phys.* 114, 2259 (2001)
  - [7] G. Monaco et al., *Phys. Rev. E* 60, 5505 (1999)
  - [8] E. Pontecorvo et al., *Phys. Rev. E* 71, 011501 (2005)
  - [9] M. Kirsch et al., *Phys. Rev. Lett.* 89, 125502 (2002)
  - [10] F. Sette et al., *Phys. Rev. Lett.* 84, 4136 (2000)
  - [11] U. Balucani et al., *Phys. Rev. E* 47, 1677 (1993)
  - [12] U. Balucani et al., *J. Phys.: Condens. Matter* 8, 9269 (1996)
  - [13] A. Monaco et al., *J. Chem. Phys.* 120, 8089 (2004)
  - [14] T. Scopigno et al., *Phys. Rev. Lett.* 85, 4076 (2000)
  - [15] T. Scopigno et al., *Phys. Rev. Lett.* 89, 255506 (2002)
  - [16] T. Scopigno et al., *Phys. Rev. E* 65, 031205 (2002)
  - [17] C. Y. Liao et al., *Phys. Rev. E* 61, 1518 (2000)
  - [18] D. Bertolini and A. Tani, *Phys. Rev. E* 51, 1091 (1995)
  - [19] U. Balucani and M. Zoppi, *Dynamics of the liquid state* (Clarendon Press, Oxford 1994)
  - [20] NIST Database, <http://webbook.nist.gov/chemistry/form-ser.html>
  - [21] R. V. Gopal Rao and R. N. Joarder, *J. Chem. Phys.* 12, 4129 (1979)
  - [22] D. Bertolini and A. Tani, *Phys. Rev. E* 56, 4135 (1997)
  - [23] T. Bryk and I. Myrberg, *Condens Matter Phys.* 7, 285 (2004)